Comparison of Hydrodynamic and Rheological Properties of Dilute Solutions of a Styrene-Hydrogenated Butadiene Copolymer in Aliphatic Solvents by Light Scattering and Viscometric Techniques

P. BEZOT,*[,1] C. HESSE-BEZOT,[1] B. ELMAKOUDI,[1] B. CONSTANS,[2] D. FAURE,[2] and P. HOORNAERT[2]

[1]Laboratoire Physique de la Matière Condensée (URA CNRS 190), Parc Valrose, BP 71, 06108 Nice, Cedex, France and [2]ELF ANTAR FRANCE, Centre de Recherche ELF, BP 22, 69360 St. Symphorien, D'Ozon, France

SYNOPSIS

Dilute solutions of a styrene-hydrogenated butadiene copolymer, a viscosity index improver, were studied by static and dynamic light-scattering techniques. In n-hexane (a model solvent for paraffinic oils) and a mineral base oil, aggregation is observed below 30°C. In cyclohexane (a model solvent for napthenic oils) only isolated polymers are present in the whole temperature range.

Kinematic viscometric measurements from 20 to 60°C in the mineral oil show a continuous increase of the intrinsic viscosity together with a decrease of k_H, the Huggins coefficient, from 2.5 to 0.5. At shear rates between 5000 and 40000 s^{-1}, a large shear thinning is observed at room temperature for the polymer in the mineral base oil. This effect progressively disappears as the temperature increases and the suspension becomes Newtonian near 100°C. All results can be interpreted in terms of micelle formation. © 1994 John Wiley & Sons, Inc.

INTRODUCTION

Understanding the relationship between polymer behavior in solution and the viscosity at various shear rates is of fundamental[1] and practical[2] importance. Various high molecular weight polymeric materials are often added as viscosity improvers[3] in numerous lubricants that are generally paraffinic molecules. It is known[2] that at low temperature the lubricant viscosity has to be low at low and intermediate shear rates whereas at high temperature it must not decrease too much at very high shear rates. Furthermore, in appropriate solvents and under particular concentration and temperature conditions, diblock copolymers tend to associate in micelles.[4] What is the impact of these associations on the viscosity value at various shear rates?

The aim of this article is not to give an answer to this question but to present a study of a particular viscosity index improver that belongs to the family of styrene-hydrogenated butadiene (SHB) copolymer that is often used in formulated industrial lubricants.

In this work, the dynamic light-scattering technique (DLS) has been used to study the hydrodynamic radius variation of the SHB polymer as a function of temperature in various solvents. Three aliphatic solvents, representative of different base oil types have been chosen. Cyclohexane and n-heptane are representative of napthenic and paraffinic oils, respectively, and 130NS Fawley is a classical base oil with a low level of aromatic components. The angular dependence of the static light scattered by the polymers in n-heptane and 130NS solvents is also measured and compared with the DLS results.

The kinematic and dynamic viscosity techniques have been run for the polymer in 130NS solvent. The shear viscosity at various shear rates measured by these methods is of great industrial interest be-

* To whom correspondence should be addressed.

Journal of Applied Polymer Science, Vol. 51, 1715–1725 (1994)
 CCC 0021-8995/94/101715-11

cause, for instance in lubricated contacts, it is directly related to the film thickness.[5] The comparison of these techniques with the DLS results is very important as this latter technique gives information on suspension in equilibrium conditions that can further the understanding of results obtained in shear experiments.[6]

EXPERIMENTAL

Materials

Suspension of SHB copolymer in a base oil at 10% g/g was purchased from Lubrizol Co. under the trade mark LZ 7440. Its architecture is intermediate between a statistical and a diblock copolymer. The weight-average molecular weight (M_w = 128000 g/mol) and the polydispersity (M_w/M_n = 1.4, where M_n is the number-average molecular weight) have been obtained against polystyrene standards by means of gel permeation chromatography (GPC) in 1,2,4-trichlorobenzene at 135°C utilizing a Waters GCP instrument.

Cyclohexane (Fluka, puriss.) and *n*-heptane (Fluka, for UV spectroscopy) were directly used after filtration through 0.2-μm pore size filters (Acrodisc Gelman 13CR, PTFE) to remove dust. The 130NS base oil is characterized by kinematic viscosities equal to 25.45 cst at 40°C and 4.68 cst at 100°C, respectively, a density equal to 0.8674 g/cm^3 at 15°C. It is mainly a paraffinic oil with 4% of total aromatic carbons.

Sample Preparation

Solutions in cyclohexane, obtained by directly diluting the base oil suspension, were filtered through a 0.2-μm pore size filter into dust-free scattering cells.

Samples in *n*-heptane were prepared from the base suspension by dialysis and were diluted before filtration through a 0.2-μm pore size filter into dust-free scattering cells.

Solutions in 130NS were prepared by dissolving the base polymer suspension in the 130NS oil at 60°C. Agitation at 80°C during 1 h was required before filtration at 60°C under a 1-μm pore size filter.

The refractive index of the three different solvents was measured with an Abbe type refractometer over a large range of temperatures. From these results, the density variation as a function of temperature has been deduced using a density value at a reference temperature and the Lorenz–Lorenz formula.

Light Scattering

A standard laboratory-built light-scattering spectrometer was used. The laser source (Coherent Innova 90-3) was operated at 514.5 nm with an output power from 0.1 to 0.5 W and the scattering angle was continuously variable from 20 to 150°. The scattering cell, put into an index-matching liquid, was temperature regulated by a circulating fluid whose temperature was stable within 0.2°C. The index-matching liquid (*o*-xylene) was filtered when necessary with a 0.2-μm pore size filter connected to a peristaltic pump.

For the DLS experiments, the main optical assembly was composed of a 150-mm focal length lens and two pinholes calculated to detect nearly one coherence area. In the case of static measurements, the pinhole in the image plane was changed for a slit. This arrangement significantly reduces errors introduced by the angular variation. The photomultiplier (EMI 9563) was selected for its low amount of afterpulsing. The autocorrelation functions (ACF) were performed with a 1096 Langley Ford Coulter multitau correlator and intensity measurements were performed with an independent photon counting system (ORTEC, 100 MHz).

The normalized second-order ACF of the scattered light intensity, $g^{(2)}(\tau)$, is related to the first-order one by:

$$g^{(2)}(\tau) = BG\{1 + A[g^{(1)}(\tau)]^2\} \qquad (1)$$

where BG is the base line that can be computed from the counters or measured at long time delay and A is related to the coherence area number. In our experiments, it was advantageous to use the multitau function of the correlator that provides a logarithmic time scale. All the ACFs recorded in the correlator memory are transferred into an IBM-PC computer for further analysis.

For a polydisperse system,

$$g^{(1)}(\tau) = \int G(\Gamma)\exp(-\Gamma\tau)\, d\Gamma, \qquad (2)$$

where the $G(\Gamma)$ is the distribution function of decay rate Γ related to the translational diffusion coefficient D by,

$$\Gamma = k^2 D, \qquad (3)$$

and where k is the scattering vector ($k = 4\pi n \sin(\theta/2)/\lambda$), n is the refractive index of the solution, θ the analysis angle, and λ the laser wavelength.

Through the Stokes–Einstein relation and assuming that the particles are noninteracting, the hydrodynamic particle radius R can be computed as,

$$R = k_B T/(6\pi\eta D), \tag{4}$$

where k_B is the Boltzmann constant, η the solvent viscosity, and T the temperature. To compute the $G(\Gamma)$, eq. (2) must be inverted. We have performed this inversion by linearizing (2),

$$g_1(\tau) = \sum_{i=1}^{N} a_i \exp(-\Gamma_i \tau). \tag{5}$$

The N values of Γ are spaced on a logarithmic scale between Γ_{min} and Γ_{max}. Moreover an additional term corresponding to $\Gamma_i = 0$ is added to expression (5) to account for dust. The a_i values, related to the scattered intensity by the particle i, are computed with the nonnegative least-squares algorithm proposed by Stock and Ray.[7]

The different distribution functions are related by,

$$\begin{aligned} a_i &= \Delta\Gamma_i G(\Gamma_i) = \Delta R_i G_I(R_i) = M_i R_i^3 P(\theta) \\ &= \Delta R_i G_w(R_i) R_i^3 P(\theta) \end{aligned} \tag{6}$$

where $G_I(R_i)$ and $G_w(R_i)$ are the intensity and weight distribution functions, M_i the weight of particles of radius between R_i and R_{i+1}, and $P(\theta)$ the form factor. Because in our experiments, $kR < 1$, the Rayleigh–Gans–Debye formula[8] can be used,

$$P(\theta) = \{3[\sin(kR) - kR\cos(kR)]/k^3R^3\}^2. \tag{7}$$

Note that relation (6) shows that the factor R^3 between the intensity and weight distributions leads to a large enhancement of the smallest particles in the weight distribution.

For each of the p populations revealed by the distribution functions, mean diameters corresponding to intensity and weight-averaged distributions, $\Phi_{I,p}$ and $\Phi_{w,p}$, respectively, are calculated according to,

$$\Phi_{I,p} = \frac{\sum_{i=N_p}^{N'_p} a_i \Phi_i}{\sum_{i=N_p}^{N'_p} a_i} \quad \text{and} \quad \Phi_{w,p} = \frac{\sum_{i=N_p}^{N'_p} M_i \Phi_i}{\sum_{i=N_p}^{N'_p} M_i} \tag{8}$$

where $(N'_p - N_p)$ is the width of the population function p and $\Phi_i = 2R_i$.

Viscometry

The kinematic viscosity measurements were performed with three capillary Ubbelohde viscometers. The range of viscosity covered extends from 0.4 to 180 cst and kinetic energy corrections were made when necessary. The temperature stability of the bath is within 0.1°C.

The dynamic viscosity measurements at shear rates extending from 5000 to 40000 s^{-1} were carried out with the Haake RV20 Rotovisco, composed of the M10 measuring head together with the HS1 sensor system. The temperature was varied over a large range with a thermal liquid circulator and particular attention was paid to verify that no local heating was present at the highest measured torques.

RESULTS AND DISCUSSION

Light-Scattering Studies

Dynamic Light Scattering

All the ACF were recorded at three θ angles (45, 90, and 135°) but no detectable angular variation was observed in the different solvents. The relatively large polydispersity of the polymer could mask some small effects due, for example, to intermolecular interactions or to the structure factor of large particles that in our case will be neglected.

Cyclohexane Solutions. The ACF were recorded at different temperatures from 20.3 to 57.8°C for a sample whose polymer concentration is $C = 10^{-3}$ g/g. The intensity distribution is composed of a main population peak of small size particles and a secondary less intense one of larger particles. Both the size and intensity of this last population decrease with increasing temperature.

The weight distribution functions, deduced from the intensity distribution functions, are shown in Figure 1. Only one population of small particles is now observable, whose mean diameter is 17 nm with a small standard deviation (σ = 3 nm). This small size, which decreases slightly with temperature, is certainly that of isolated polymers.

n-*Heptane Solutions.* The ACF have been recorded at four temperatures ranging from 20 to 78.2°C for a sample whose polymer concentration is $C = 4 \quad 10^{-4}$ g/g or $2.7 \quad 10^{-4}$ g/cm^3 at 20°C.

The intensity distribution function is characterized by a large temperature variation. The mean diameters computed from the various intensity populations are reported in the left-hand side of Table

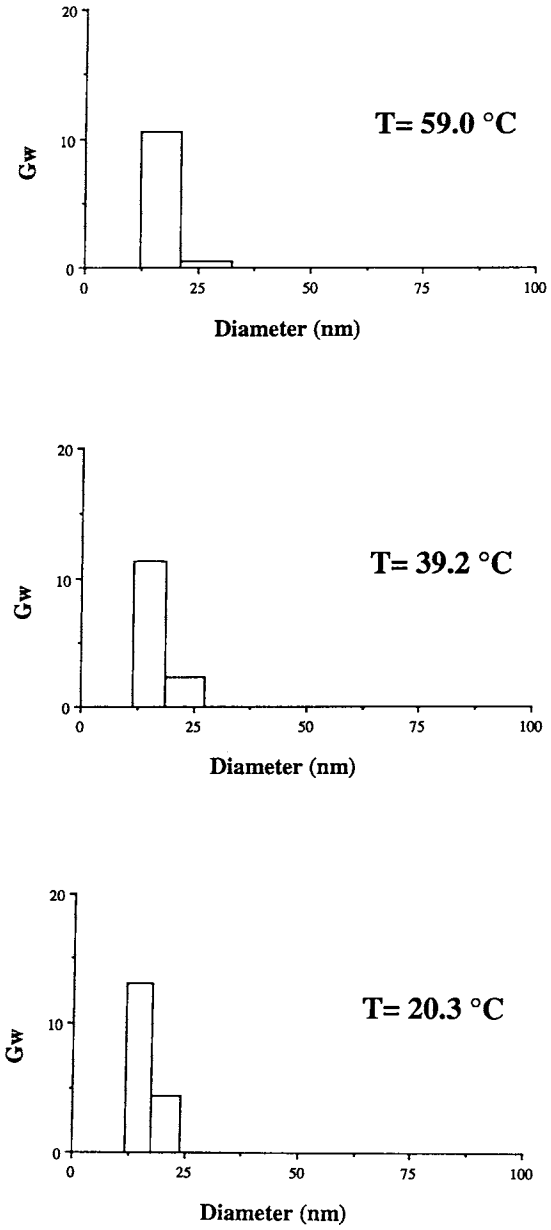

Figure 1 Weight distribution function of particle size, G_w in arbitrary unit, for SHB copolymer in cyclohexane as a function of temperature.

I. At room temperature, only one population centered near 70 nm is present. From 40 to 78°C, a continuously increasing population of small particles is present. This population is centered at 16 nm with a polydispersity that narrows at 78°C.

The results for the weight distribution functions and the corresponding mean diameters are reported in Figure 2 and on the right-hand side of Table I. At 20.3°C, the whole quantity of polymer is concentrated in only one large size population. However, over a range of less than 20°C, more than 90% of the polymer weight is gathered in a small size population with a relatively large polydispersity. As the temperature rises to 78.2°C, only one narrow peak for particles of small size exists in the distribution and certainly corresponds to the isolated polymer.

Other measurements made on more concentrated solutions lead to roughly the same behavior.

130NS Solutions. The ACF were measured at six temperatures ranging from 20.3 to 90.6°C for a solution with a polymer concentration $C = 1\ 10^{-2}$ g/g.

The intensity distribution functions are characterized by a variation particularly significant above 70°C. The computed mean diameters are reported in the left-hand part of Table II. Below 80°C, only one peak is observed and the mean size slightly increases with increasing temperature; simultaneously its polydispersity decreases. Above 80°C, a second peak for small size particles appears and becomes dominant near 90°C; that is the temperature at which the large particles have totally disappeared.

The results obtained on the weight distribution functions and corresponding mean diameters are reported in Figure 3 and Table II. Below 80°C all polymers are gathered in relatively large particles whose diameter varies from 64 to 76 nm when the temperature increases from 20.3 to 80.3°C. Above this latter temperature, these large size particles disappear and transform into small size ones with a very small polydispersity.

Table I Mean Diameter, Standard Deviation, and Fraction of Different Populations Computed for SHB Copolymer in *n*-Heptane With $C = 4.0\ \ 10^{-4}$ g/g

	Intensity Distribution					Weight Distribution				
T (°C)	Φ_1 (nm)	σ_1 (nm)	I_1 (%)	Φ_2 (nm)	I_2 (%)	Φ_1 (nm)	σ_1 (nm)	I_1 (%)	Φ_2 (nm)	I_2 (%)
20.3	—	—	—	73	100	—	—	—	73	100
39.3	17	4	12	67	88	14	4	93	66	7
57.8	16	3	75	60	25	16	3	100	—	—
78.2	16	1	100	—	—	16	1	100	—	—

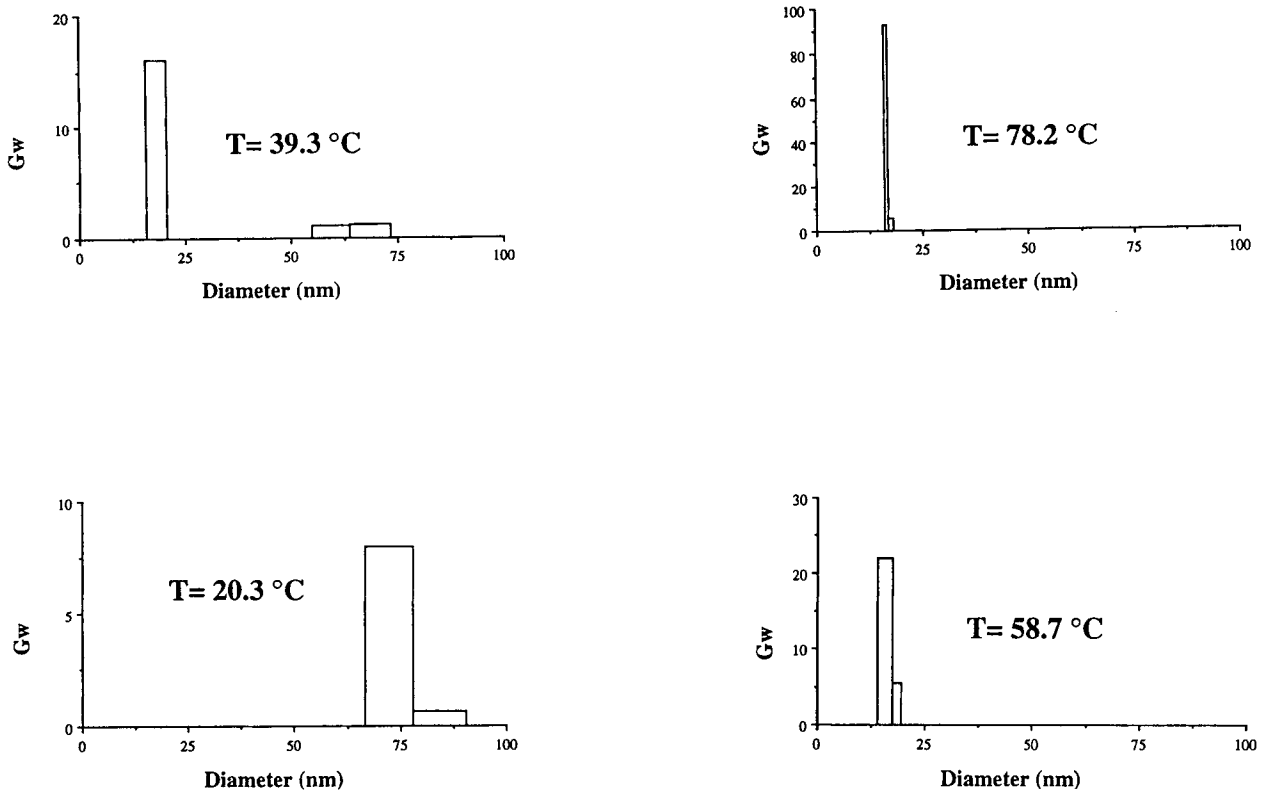

Figure 2 Weight distribution function of particle size, G_w in arbitrary unit, for SHB copolymer in n-heptane as a function of temperature.

Static Light Scattering

The scattered intensity was recorded at three θ angles (135, 90, and 45°) as a function of temperature, at concentrations $C = 10^{-2}$ g/g in 130N and $C = 4 \quad 10^{-3}$ g/g in n-heptane. Over the whole temperature range the scattered intensity, corrected by the scattering volume term sin θ, has no angular dependence. The corresponding normalized mean value is reported in Figure 4 for n-heptane and 130NS solutions as a function of temperature.

In both solutions, as the temperature varies, the scattered intensity decreases. Moreover, the intensity reaches its minimum value at a lower temperature in the case of the n-heptane solution.

The theoretical prediction of the intensity[9] is,

$$I\alpha(NV)V\frac{(n_1^2 - n_2^2)^2}{(n_1^2 + 2n_2^2)^2}S(k) \qquad (9)$$

where N is the number of particles, V its volume, n_1 the particle refractive index ($n_1 \approx 1.5$ for poly-

Table II Mean Diameter, Standard Deviation, and Fraction of Different Populations Computed for SHB Copolymer in 130NS Base Oil With $C = 1.0 \quad 10^{-2}$ g/g

	Intensity Distribution					Weight Distribution				
T (°C)	Φ_1 (nm)	σ_1 (nm)	I_1 (%)	Φ_2 (nm)	σ_2 (nm)	Φ_1 (nm)	σ_1 (nm)	I_1 (%)	Φ_2 (nm)	I_2 (%)
20.3	—	—	0	68	13	—	—	0	64	100
38.4	—	—	0	74	15	—	—	0	72	100
62.0	—	—	0	74	8	—	—	0	72	100
68.8	—	—	0	76	8	—	—	0	76	100
80.3	17	4	39	75	8	16	4	98	75	2
90.6	18	3	100	—	—	17	3	100	—	—

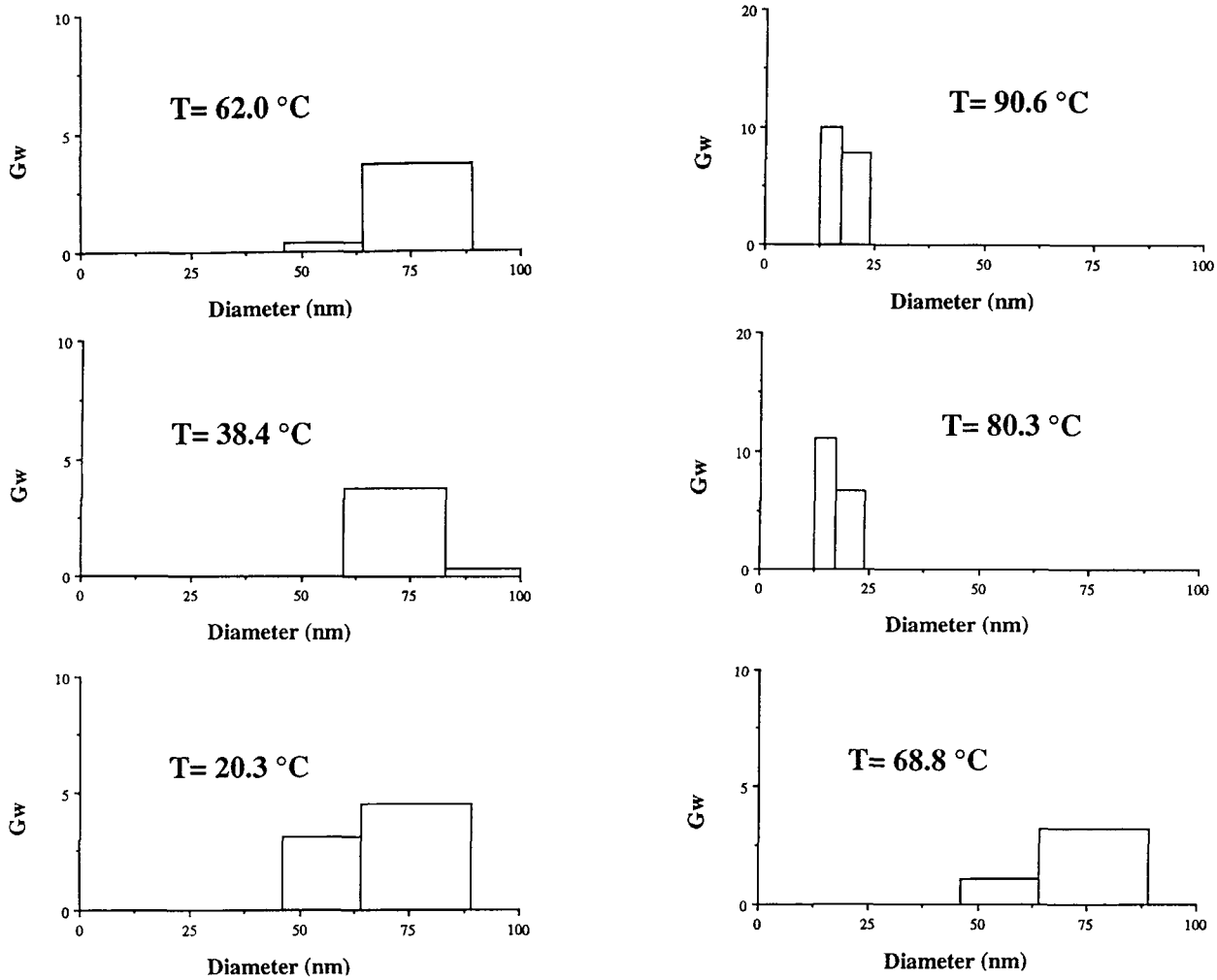

Figure 3 *Weight distribution function of particle size, G_w in arbitrary unit, for SHB copolymer in 130NS base oil as a function of temperature.*

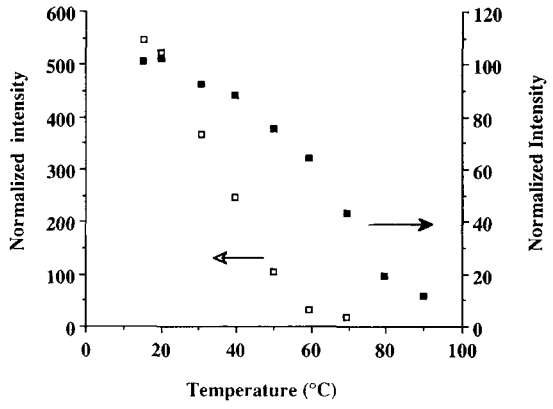

Figure 4 Plot of mean normalized scattering intensity for SHB copolymer (□) in *n*-heptane and (■) in 130NS base oil as a function of temperature.

mers), n_2 the solvent refractive index, and $S(k)$ the structure factor for the analysis wave vector k.

In this expression, for a given quantity of matter, the NV term can be considered as a constant. The main intensity variation comes from the V term that strongly depends on the particle size R. Consequently, as the DLS results show a large decrease of the mean particle size, the corresponding scattered intensity must also decrease. At about 60°C for *n*-heptane and 80°C for 130NS solutions, the scattered intensity reaches its minimum value when only isolated polymers are present (Figs. 2, 3). The third term (contrast) is related to the n_1/n_2 ratio. In the case of 130N ($n_2 \approx 1.48$) solutions this ratio is close to 1. Conversely, in *n*-heptane ($n_2 \approx 1.37$) solutions this ratio is larger than 1. This explains why, even

for a lower concentration, the scattered light of the *n*-heptane solution is larger than for the 130NS one. The $S(k)$ factor depends on the kR value and is equal to 1 for small values of kR. No θ or k dependence has been observed and hence this means that the radius of the particle is less than $\lambda/10$ in agreement with our DLS results.

Comments

It is clear that, in the three kinds of suspensions under study in the present article, the SHB copolymers are gathered in two kinds of populations: one composed of small size particles whose diameter ($\approx$ 17 nm) corresponds nearly to that of the isolated polymers and a second that is a result of polymer association.

In the case of diblock copolymer, it is known that under particular conditions, polymers can associate to form micelles[10,11] of which the central core consists of blocks immiscible in the solvent and the outer corona is composed of soluble blocks swollen by the solvent.

Due to its architecture, SHB will have some properties of diblocks copolymers and we expect micellization under certain temperature and solvent conditions, not necessarily the same as for pure diblock copolymers.

It is known that cyclohexane is a good solvent for hydrogenated polybutadiene and, above 34°C, changes from θ to good solvent for the polystyrene.[12] Below this temperature, because SBH is intermediate between diblock and statistical copolymer, we can expect that no aggregation will be observed down to 20°C. Our experimental results on cyclohexane suspensions are in good agreement with this assumption because from 20.3 to 57.8°C, all polymers are found to have only one single small size population peak that corresponds to the isolated polymer.

In *n*-heptane and 130N solvents, the polymer behavior is very different: at room temperature polymers are clustered and it is likely that these clusters ($\Phi \approx$ 70 nm) are micelles. In agreement with this behavior, it has been recently observed[13] that (styrene–butadiene) block copolymers associate in *n*-decane solvent and form micelles. It is reasonable to suppose that, at room temperature, *n*-heptane and 130N are poor solvents for polystyrene and, as they are good solvents for hydrogenated butadiene, micelles with a central core consisting of polystyrene blocks are likely to form.

As the temperature is increased, clusters are observed to change into isolated polymers. The temperature at which this modification happens is higher for 130N than for *n*-heptane.

The reasons for this cluster disaggregation are still not totally clear to us. However, we think that they could be related to the temperature variation of the critical micellar concentration (CMC) without any change of the solvent quality as observed for polystyrene-block-poly(ethylene-propylene) copolymer in hexane by Quintana et al.[14,15] They found that the CMC varies by a factor larger than 10^5 from 25 to 86°C. So it is possible that as the temperature increases, the CMC becomes higher than the concentrations under study.

To verify this hypothesis, two very dilute solutions were studied. For the lowest concentration ($C = 2.710^{-6}$ g/cm^3), the scattered intensity was very low and DLS measurements indicate that at 20°C only isolated polymers are present. The results for $C = 2.710^{-5}$ g/cm^3 or 4 10^{-5} g/g are reported in Table III. They show that at 20°C only clusters have been detected which totally disaggregate at 40°C. So we can conclude that for this polymer the CMC is lower than 2.710^{-5} g/cm^3 and higher than 2.710^{-6} g/cm^3 at 20°C and becomes higher than 2.710^{-4} g/cm^3 at 40°C (Table I).

However, in the case of *n*-heptane, if we compare our values at 20°C with the CMC found by Quintana, it appears that our values are slightly high. But as the polymers are not the same, this discrepancy

Table III Mean Diameter, Standard Deviation, and Fraction of Different Populations Computed for SHB Copolymer in *n*-Heptane With $C = 4.0$ 10^{-5} g/g

	Intensity Distribution					Weight Distribution				
T (°C)	Φ_1 (nm)	σ_1 (nm)	I_1 (%)	Φ_2 (nm)	I_2 (%)	Φ_1 (nm)	σ_1 (nm)	I_1 (%)	Φ_2 (nm)	I_2 (%)
20.3	—	—	—	70	100	—	—	—	70	100
39.3	13	2	100	—	—	13	2	100	—	—
57.8	16	1	100	—	—	16	1	100	—	—

could be explained by a more negative value of ΔH and/or a less negative ΔS. If, moreover, the solvent quality varies with temperature, ΔH and ΔS cannot be considered as constants.

In the 130N solvent, comparison with the literature is more difficult. We can only say that the CMC decreases with the carbon number of alkanes.[15] This could explain why, in this solvent, the isolated polymers appear at higher temperature than in n-heptane.

Viscometry Measurements

Kinematic Viscosity

The measurements were made on solutions at concentration between $C = 0.1$ and 2.5% g/g in 130NS solvent within a temperature range from 20 to 100°C.

For concentrations lower than 1% g/g, the Huggins expression[16] for the reduced viscosity η_{sp}/C,

$$\eta_{sp}/C = [\eta] + k_H[\eta]^2 C, \qquad (10)$$

was found to correctly fit the experimental values. In this expression, $[\eta]$ is the intrinsic viscosity and k_H, the Huggins' coefficient. The values of $[\eta]$ and k_H are reported in Figure 5.

$[\eta]$ is observed to increase when temperature varies from 40 to 60°C and then decreases above 80°C. The Huggins coefficient varies in the opposite sense to the intrinsic viscosity in the same temperature range.

These results are to be compared with the DLS measurements that indicate clearly that at low temperature the polymers are clustered in a single population of micelles. If the micelle is modeled by a hard sphere, the intrinsic viscosity is given by the Einstein relation,[17]

$$[\eta] = 2.5 \quad 4/3\pi R^3 N_A/M_c$$
$$= 6.3 \quad 10^{24} R^3/M_c \qquad (11)$$

where the 2.5 factor is the Einstein coefficient for a sphere, $4/3\pi R^3$, its volume being V and M_c/N_A, its weight m. $[\eta]$ is proportional to the ratio V/m and consequently related to the compactness of the micelles. Figure 5 shows that within experimental errors and below 40°C, the micelle volume does not depend on temperature. From the DLS values of the micelle radius ($R \approx 35$ nm) and the intrinsic viscosity ($[\eta] = 40$ cm^3/g) the micellar molar mass is found to be equal to 6.7 10^6 g/mol. Consequently the number of polymer units in a micelle is about 50, in good agreement with values obtained for styrene–butadiene copolymer in n-decane solvent.[13]

At high temperature, the DLS shows that all micelles are transformed into isolated polymers. In this case, which is more complicated, many expressions are proposed in the literature to calculate the intrinsic viscosity.[18] For instance in the Fox and Flory theory,[19]

$$[\eta] = \Phi R_G^3/M_p \qquad (12)$$

where R_G is the mean value of the radius of gyration related to the polymer expansion, M_p its molecular weight, and Φ a universal constant independent of polymer, solvent and temperature and equal to 5.3 10^{24} in the case of a Gaussian coil. At 90°C, from relation (12), we found $R_g \approx 11$ nm. This can be compared to the hydrodynamic value ($Rh \approx 8.5$ nm) and confirms that only isolated polymers are present in the suspension at 90°C.

As the constant terms in eqs. (11) and (12) are nearly equal, it is likely that the large variation of intrinsic viscosity, observed between low and high temperature, can be attributed to a compactness difference between micelles and isolated polymers. Furthermore the gradual enhancement of the intrinsic viscosity between 20 and 80°C is probably due to the progressive increase of the number of isolated polymers.

Above 80°C, the intrinsic viscosity is observed to decrease. As the molecular weight of the polymer is constant, this variation can be attributed to a de-

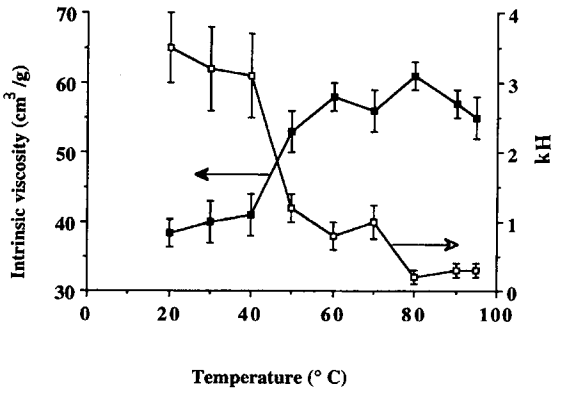

Figure 5 Intrinsic viscosity and Huggins' coefficient, k_H, for SHB copolymer in 130NS base oil as a function of temperature.

crease of the polymer expansion coefficient, related to the modification of the solvent goodness.

It is worth noting that generally, in the petroleum companies, standard measurements are made at 40 and 100°C that in our case could lead to an erroneous idea of the fluid behavior between these two limiting temperatures.

Figure 4 shows that the k_H coefficient varies, as already observed,[6] in the opposite sense to the intrinsic viscosity. It rises up to 3 ± 0.5 and decreases to a value smaller than 0.5, the mean value generally found for isolated polymers in solution. The large k_H value generally indicates the presence of micelles in the suspension.[20]

The reduced viscosity values, obtained on a large range of concentration up to 2.5% g/g are reported in Figure 6. It is observed that, at high temperature, the Huggins expression describes correctly all the experimental results. However, at low temperature, the concentration dependence of the reduced viscosity becomes concave upward, which is a consequence of the micelle formation.

Dynamic Viscosity

The reduced viscosity values η_{sp}/C are reported in Figure 7 at 40°C as a function of concentration from 0.1 to 2.5% g/g at various shear rates from 8640 to 40000 s^{-1}. In the same figure, the reduced viscosity values from kinematic measurements are also shown. The observed shear thinning is greater at higher concentration and consequently, at high shear rate the resulting reduced viscosity becomes linear as a function of concentration.

Figure 8 details the behavior of the specific viscosity η_{sp} at two particular concentrations (1 and 2.5% g/g) as a function of shear rate. It appears that the critical shear rate at which the fluid becomes non-Newtonian is a decreasing function of the concentration. These results are in agreement with those obtained by Hassanean and Bartz[21] with the same polymer diluted at 2.47 and 1.8% g/g in a pure base oil similar to the 130NS and reported in Figure 8. Moreover a similar behavior has been observed by Kulicke and Kniewske[22] for polystyrene samples of various molecular weights from 0.33 to 23×10^6 g/mol dissolved in toluene at concentrations varying from 0.5 to 4% g/g. The critical shear rate, measured in our sample at 2.5% g/g, corresponds to a polystyrene molecular weight larger than 10^6 g/mol, which is in agreement with an estimated value of the micelle molar weight.

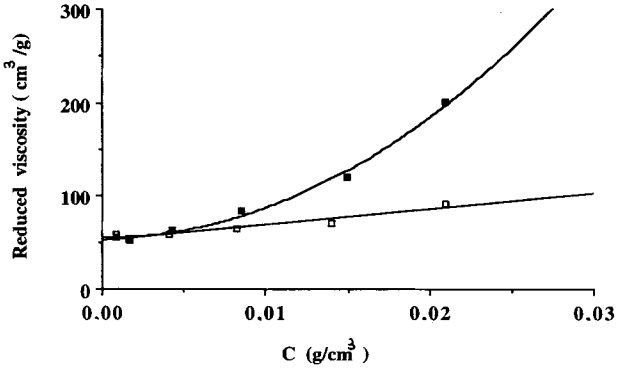

Figure 6 Reduced viscosity for SHB copolymer in 130NS base oil at (■) 20°C and (□) 90°C as a function of concentration.

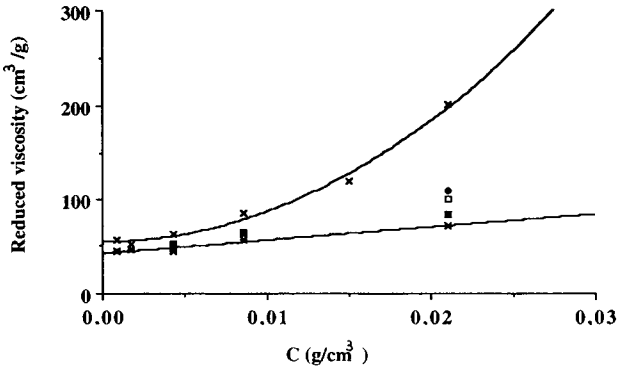

Figure 7 Reduced viscosity for SHB copolymer in 130NS base oil for different shear rates: (*) 40000 s^{-1}; (■) 24000 s^{-1}; (□) 14360 s^{-1}; (♦) 8640 s^{-1}) and (×) kinematic value as a function of concentration.

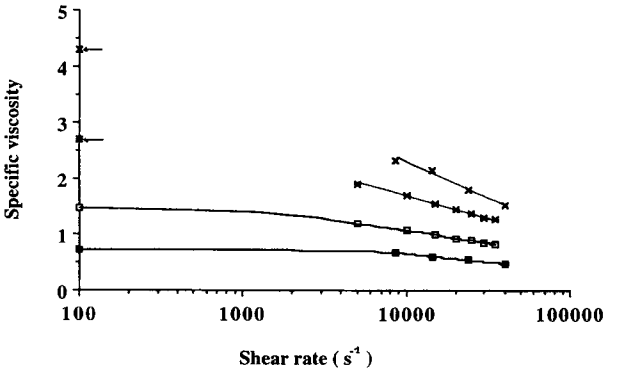

Figure 8 Specific viscosity for SHB copolymer in 130NS base oil with (■) C = 1% g/g and (×) C = 2.5% g/g as a function of shear rate. Comparison with values from Hassanean and Bartz[21] with (*) C = 2.47% g/g and (□) C = 1.8% g/g in a nonformulated base oil.

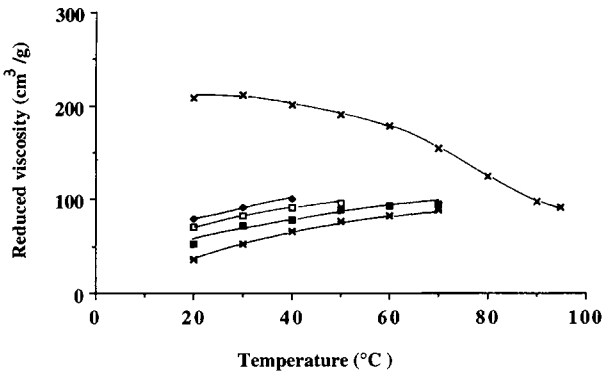

Figure 9 Reduced viscosity for SHB copolymer with C = 2.5% g/g in 130NS base oil for various shear rates: (*) 40000 s^{-1}; (■) 24000 s^{-1}; (□) 14360 s^{-1}; (♦) 8640 s^{-1}) and (×) kinematic value as a function of temperature.

Figure 9 shows the reduced viscosity values of the 2.5% g/g solution as a function of temperature at various shear rates. The shear thinning is observed to decrease with the temperature and becomes smaller than the experimental errors above 80°C. The same results were obtained by Hassanean and Bartz[21] who observed at 100°C a Newtonian behavior from 100 to 35000 s^{-1}. At 80°C or higher, only isolated polymers of smaller molecular weight (M_w = 128000 g/mol) are present in the solution. Consequently the critical shear rate becomes larger than 40000 s^{-1} as was also observed with polystyrene of different molecular weights.[22] Because between 50 and 80°C, polymers and micelles are present in various proportions in the suspension, results in this intermediate range become more difficult to interpret.

Note that Figure 9 shows clearly that the reduced viscosities at high and low shear rates have opposite temperature dependence. This behavior means that high shear rates lead to an enhancement of the thickening effect as the temperature increases. This result is of importance for lubrication.

Comments

At 80°C or higher, all viscometric results in the 130NS solvent are in agreement with the known behavior of isolated polymers of low molecular weight. The Huggins relation fits the experimental results correctly with a k_H value of about 0.5 and no shear rate effect up to 40000 s^{-1} is detected.

At 40°C a large shear thinning is observed and simultaneously the k_H coefficient becomes large. All these results can be interpreted by the presence of micelles.

In the intermediate temperature range, the suspension contains both micelles and isolated polymers. So the shear thinning is already present and the intrinsic viscosity increases with temperature along with a decrease of k_H.

CONCLUSIONS

The present study of an SHB copolymer diluted in three different aliphatic solvents has shown that the polymer behavior depends on solvent nature and temperature.

At high temperature, all the measurements prove the existence of only isolated polymers in the different samples under study.

Conversely at room temperature, only micelles are observed in n-heptane and 130NS base oil whereas in cyclohexane isolated polymers are still present. This is in agreement with the diblock nature of the SHB in which the styrene and the hydrogenated butadiene each have different affinity for n-heptane and 130NS whereas cyclohexane is a good solvent for the two blocks from 20 to 60°C.

We have shown that this hydrodynamic behavior leads to a large modification of the rheological properties of the suspension as a function of temperature. This result is of great importance for industrial applications.

We gratefully acknowledge financial support of this research work by SNEA Company (Elf Antar France, CR 8282). We thank Mrs. C. Laye for her technical assistance.

REFERENCES

1. M. Doi and S. F. Edwards, *The Theory of Polymer Dynamics,* Clarendon Press, Oxford, 1986.
2. J. Briant, J. Denis, and G. Parc, *Rheological Properties of Lubricants,* Technip, Paris, 1985.
3. D. N. Schulz and J. E. Glass, *Polymers as Rheology Modifiers,* American Chemical Society, Washington, D.C., 1991.
4. Z. Tuzar and P. Kratochvil, *Adv. Colloid Interface Sci.,* **6,** 201 (1976).
5. B. J. Hamrock and D. Dowson, *Ball Bearing Lubrication,* Wiley, New York, 1981.
6. E. Maderek and B. A. Wolf, *Angew. Makromol. Chem.,* **161,** 157 (1988).
7. R. S. Stock and W. H. Ray, *J. Polym. Sci., Polym. Phys. Ed.,* **23,** 1393 (1985).

8. B. J. Berne and R. Pecora, *Dynamic Light Scattering,* Wiley, New York, 1976.
9. M. Kerker, *Scattering of Light,* Academic Press, New York, 1969.
10. J. Plestil and J. Baldrian, *Makromol. Chem.,* **176,** 1009 (1975).
11. F. Candau, F. Heatley, C. Price, and R. Stubbersfield, *Eur. Polym. J.,* **20,** 685 (1984).
12. B. K. Varma, Y. Fujita, M. Takahashi, and T. Nose, *J. Polym. Sci., Polym. Phys. Ed.,* **22,** 1781 (1984).
13. Y. Tsunashima, M. Hirata, and Y. Kawamata, *Macromolecules,* **23,** 1089 (1990).
14. J. R. Quintana, M. Villacampa, M. Munoz, A. Andrio, and I. A. Katime, *Macromolecules,* **25,** 3125 (1992).
15. J. R. Quintana, M. Villacampa, A. Andrio, M. Munoz, and I. A. Katime, *Macromolecules,* **25,** 3129 (1992).
16. M. L. Huggins, *J. Am. Chem. Soc.,* **64,** 2716 (1942).
17. A. Einstein, *Ann. Physik,* **19,** 289 (1906); **34,** 591 (1911).
18. P. J. Flory, *Principles of Polymer Chemistry,* Chap. 8, Cornell Univ. Press, Ithaca, NY, 1953.
19. (a) T. G. Fox and P. J. Flory, *J. Phys. Colloid. Chem.,* **53,** 197 (1949); (b) P. J. Flory, *J. Chem. Phys.,* **17,** 303 (1949).
20. A. S. Yeung and C. W. Frank, *Polymer,* **31,** 2089 (1990).
21. M. H. M. Hassanean and W. J. Bartz, *Tribology 2000,* Vol. 1, 3-3.1, W. J. Bartz, Ed. 8th International Colloquium (14–16 January 1992), Technische Akademie Esslingen.
22. W. M. Kulicke, R. Kniewske, *Rheologica Acta,* **23,** 75 (1984).

Received May 29, 1993
Accepted August 1, 1993